

Toward Robust Neural Networks via Sparsification

Soorya Gopalakrishnan*, Zhinus Marzi*, Upamanyu Madhow, Ramtin Pedarsani

University of California, Santa Barbara

{soorya, zhinus_marzi, madhow, ramtin}@ucsb.edu

Abstract

It is by now well-known that small *adversarial* perturbations can induce classification errors in deep neural networks. In this paper, we make the case that a systematic exploitation of sparsity is key to defending against such attacks, and that a “locally linear” model for neural networks can be used to develop a theoretical foundation for crafting attacks and defenses. We consider two defenses. The first is a sparsifying front end, which attenuates the impact of the attack by a factor of roughly K/N where N is the data dimension and K is the sparsity level. The second is sparsification of network weights, which attenuates the worst-case growth of an attack as it flows up the network. We also devise attacks based on the locally linear model that outperform the well-known FGSM attack. We provide experimental results for the MNIST and Fashion-MNIST datasets, showing the efficacy of the proposed sparsity-based defenses.

1 Introduction

Since Szegedy et al. (2014) and Goodfellow et al. (2015) pointed out the vulnerability of deep networks to small *adversarial* perturbations, there has been an explosion of research effort in adversarial attacks and defenses. In this paper, we attempt to provide fundamental insight into both the vulnerability of deep networks to carefully designed perturbations, and a systematic, theoretically justified framework for designing defenses against adversarial perturbations.

Our starting point is the original intuition in Goodfellow et al. (2015), validated by other recent work (Moosavi-Dezfooli et al., 2016; Fawzi et al., 2017; Poole et al., 2016), that deep networks are vulnerable to small perturbations not because of their complex, nonlinear structure, but because of their being “too linear”. Consider the simple example of a binary linear classifier \mathbf{w} operating on N -dimensional input \mathbf{x} , producing the decision statistic $f(\mathbf{x}) = \mathbf{w}^T \mathbf{x}$. The effect of a perturbation \mathbf{e} to the input is given by $f(\mathbf{x} + \mathbf{e}) - f(\mathbf{x}) = \mathbf{w}^T \mathbf{e}$. Now, if \mathbf{e} is bounded by ℓ_∞ norm (i.e., $\|\mathbf{e}\|_\infty = \max_i e_i \leq \epsilon$), then the largest perturbation that can be produced at the output is given by $\mathbf{e} = \epsilon \text{sgn}(\mathbf{w})$, and the resulting output perturbation is $\Delta = \epsilon \sum_{i=1}^N |w_i| = \epsilon \|\mathbf{w}\|_1$. The latter can be made large unless the ℓ_1 norm of \mathbf{w}

*Joint first authors.

is constrained in some fashion. To see what happens without such a constraint, suppose that \mathbf{w} has independent and identically distributed components, each with zero mean and variance 1. It is easy to see that $\|\mathbf{w}\|_1 = \Theta(N)$,¹ which means that the effect of ℓ_∞ -bounded input perturbations can be blown up at the output as the input dimension increases.

The preceding linear model provides a remarkably good approximation for today’s deep CNNs. Convolutions, subsampling, and average pooling are inherently linear. A ReLU unit is piecewise linear, switching between slopes at the bias point. A max-pooling unit is a switch between multiple linear transformations. Thus, the overall transfer function between the input and an output neuron can be written as $\mathbf{w}_{\text{eq}}(\mathbf{x})^T \mathbf{x}$, where $\mathbf{w}_{\text{eq}}(\mathbf{x})$ is an equivalent “locally linear” transformation that exhibits input dependence through the switches corresponding to the ReLU and max pooling units. For small perturbations, relatively few switches flip, so that $\mathbf{w}_{\text{eq}}(\mathbf{x} + \mathbf{e}) \approx \mathbf{w}_{\text{eq}}(\mathbf{x})$. Note that the preceding argument also applies to more general classes of nonlinearities: the locally linear approximation is even better for sigmoids, since slope changes are gradual rather than drastic.

These observations allow us to build on our prior work (Marzi et al., 2018), where we have shown that a sparsity-based defense is *provably* effective for *linear* classifiers. Specifically, we assume that the input data is sparse in a known basis, and employ a sparsifying front end that projects the perturbed data onto the smaller subspace. The intuition behind why sparsity can help is quite clear: small perturbations can add up to a large output distortion when the input dimension is large, and by projecting to a smaller subspace, we limit the damage. Indeed, theoretical calculations show that the impact of ℓ_∞ -bounded attacks on the output is attenuated by a factor of roughly K/N , where N is the data dimension and K is the sparsity level.

Contributions: In this paper, we extend the preceding ideas from linear classifiers to nonlinear neural networks, and show the importance of importance of both generative and discriminative approaches to sparsity in defending against adversarial attacks. Our main contributions are as follows:

- Using a “locally linear” model for neural networks, we provide a framework for understanding the impact of small perturbations, characterizing a regime in which the fraction of switches flipping for ReLU nonlinearities for an ℓ_∞ -bounded perturbation is small.
- We demonstrate that the preceding framework can be used for crafting both defenses and attacks. Specifically, we show that a sparsifying front end is effective for defense, and devise a new locally linear attack that outperforms the well-known FGSM attack. We supplement our theoretical results with experiments on simple datasets for a variety of recent attacks.
- We show that our complementary discriminative strategy of imposing sparsity *within* the neural network can be used to impose ℓ_∞ bounds on the effective perturbation seen by each layer, and report on promising preliminary experimental results.

¹See Appendix A for definitions of the order notation $\Theta(\cdot)$, $\mathcal{O}(\cdot)$, $\omega(\cdot)$, $\mathcal{o}(\cdot)$.

Related work: Some recently proposed defenses utilize preprocessing techniques that are implicitly sparsity-based, including JPEG compression (Guo et al., 2018; Das et al., 2017), PCA (Bhagoji et al., 2017) and projection onto generative models (Ilyas et al., 2017; Samangouei et al., 2018). However, their evaluations have been empirical in nature. Our goal here is to provide a theoretically grounded framework which permits a systematic pursuit of sparsity as a key tool for robust machine learning.

A different class of *provable* defenses focus on minimizing various upper bounds on the impact of adversarial perturbations, including spectral norm regularization (Cisse et al., 2017), cross-Lipschitz regularization (Hein and Andriushchenko, 2017), adaptive regularization (Ragunathan et al., 2018), training on a “dual” deep network (Wong and Kolter, 2018) and Wasserstein penalty based training procedures (Sinha et al., 2018). Our work on robustness guarantees for sparsity-based defenses supplements these as an additional tool to combat adversarial examples.

2 Overview of sparsity-based defenses

Given a neural network, we consider a system composed of two participants: the adversary and the defense. The adversary perturbs the input to the network, with the goal of causing misclassification. We are interested in perturbations that are visually imperceptible, hence we impose an ℓ_∞ -constraint on the adversary: $\|\mathbf{e}\|_\infty \leq \epsilon$. The defense modifies the classifier in order to attenuate the impact of the adversary. We consider two sparsity-based defenses (depicted in Figures 1 and 2):

- **Sparsifying front end:** This strategy exploits the rather general observation that input data must be sparse in *some* basis in order to avoid the curse of dimensionality. Specifically, we assume that input data $\mathbf{x} \in \mathbb{R}^N$ has a K -sparse representation ($K \ll N$) in an orthonormal basis Ψ :

$$\|\Psi^T \mathbf{x}\|_0 \leq K.$$

The defense pre-processes the input via a front end that enforces sparsity in Ψ . Specifically, function $\mathcal{H}_K(\cdot)$ enforces sparsity by retaining the K coefficients largest in magnitude and zeroing out the rest.

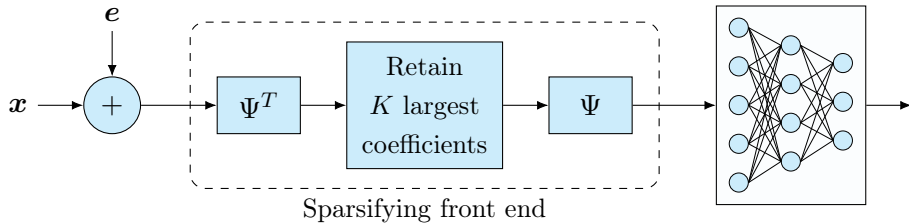


Figure 1: Sparsifying front end defense: For a basis in which the input is sparse, the input is projected onto the subspace spanned by the K largest basis coefficients. This attenuates the impact of the attack by K/N , where N is the input dimension.

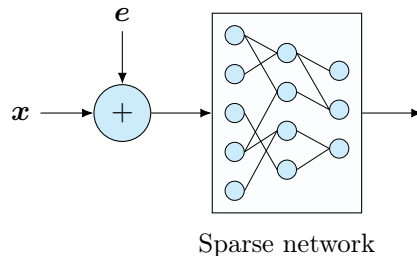


Figure 2: Network sparsity defense: Imposing sparsity *within* the neural network attenuates the worst-case growth of the attack as it flows up the network.

If the data is exactly K sparse in domain Ψ , the front end leaves the input unchanged ($\hat{\mathbf{x}} = \mathbf{x}$) when there is no attack ($\mathbf{e} = 0$). If the perturbation is small enough, then the K retained coefficients corresponding to \mathbf{x} and $\mathbf{x} + \mathbf{e}$ remain the same, in which case the neural network sees the original input plus the projected (hence attenuated) perturbation.

- **Network sparsity:** This approach imposes sparsity *within* the neural network via ℓ_1 regularization of weights at each layer. As we show in Section 4, this limits the effective layer-wise ℓ_∞ perturbation.

3 Sparsifying front ends

We begin with a brief review of sparsifying front ends for linear classifiers, and then extend the ideas to neural networks.

3.1 Background on linear classifiers

For a linear classifier, our prior work (Marzi et al., 2018) establishes a theoretical framework demonstrating the efficacy of the sparsifying front end in Figure 1. When $y(\mathbf{x}) = \mathbf{w}^T \mathbf{x}$, the distortion caused by the adversary is given by $\Delta = |\mathbf{w}^T (\hat{\mathbf{x}} - \mathbf{x})|$.

Under a high SNR assumption (where the attack does not shift the support of the K -sparse representation of \mathbf{x}), the distortion can be written as $\Delta = |\mathbf{e}^T \mathcal{P}_K(\mathbf{w}, \mathbf{x})|$, where $\mathcal{P}_K(\mathbf{w}, \mathbf{x})$ is the projection of \mathbf{w} on to the K -dimensional subspace that \mathbf{x} lies in. The adversary then attempts to maximize the distortion under the constraint $\|\mathbf{e}\|_\infty < \epsilon$. Now we can consider two settings:

- *Semi-white box:* Here the perturbations are designed based on knowledge of \mathbf{w} alone, so that $\mathbf{e}_{\text{SW}} = \epsilon \text{sgn}(\mathbf{w})$ and $\Delta_{\text{SW}} = \epsilon |\text{sgn}(\mathbf{w}^T) \mathcal{P}_K(\mathbf{w}, \mathbf{x})|$.
- *White box:* Here the adversary has knowledge of both \mathbf{w} and the front end. Assuming high SNR, the optimal perturbation is $\mathbf{e}_{\text{W}} = \epsilon \text{sgn}(\mathcal{P}_K(\mathbf{w}, \mathbf{x}))$, which yields $\Delta_{\text{W}} = \epsilon \|\mathcal{P}_K(\mathbf{w}, \mathbf{x})\|_1$.

The benchmark distortion with no front end is $\Delta = \epsilon \|\mathbf{w}\|_1$.

The efficacy of the sparsifying front end can be quantified by taking an ensemble average based on a stochastic model for \mathbf{w} . Specifically, the defense attenuates the

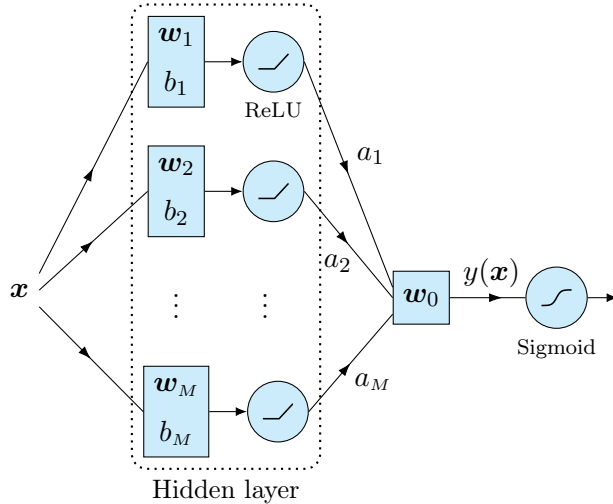


Figure 3: Two layer neural network for binary classification. ReLU units are piecewise linear, hence the network is locally linear: $y(\mathbf{x}) = \mathbf{w}_{\text{eq}}(\mathbf{x})^T \mathbf{x} - b_{\text{eq}}(\mathbf{x})$.

output distortion by a factor of K/N for the semi-white box attack, and by at least $\mathcal{O}(K \text{ polylog}(N)/N)$ for the white box attack, where K is the sparsity of the signal and N is the signal dimension.

A practical take-away from the calculations involved is that, in order for the defense to be effective against a white box attack, not only do we need $K \ll N$, but we also need that the individual basis functions be localized (small in ℓ_1 norm). The latter implies, for example, that sparsification with respect to a wavelet basis, which has more localized basis functions, should be more effective than with a DCT basis.

In the next section, we build on these insights for neural networks by exploiting locally linear approximations. For simplicity we start with a 2-layer, fully connected network trained for binary classification, and then extend our results to a general network for multi-class classification.

3.2 Neural networks: Locally linear representation

Consider first binary classification using a neural network with one hidden layer with M neurons, as depicted in Fig. 3. Since ReLU units are piecewise linear, switching between slopes of 0 and 1, they can be represented using input-dependent switches. Given input \mathbf{x} , we denote by $s_i(\mathbf{x}) \in \{0, 1\}$ the switch corresponding to the i th ReLU unit. Now the activations of the hidden layer neurons can be written as follows:

$$a_i = \text{ReLU}(\mathbf{w}_i^T \mathbf{x} - b_i) = s_i(\mathbf{x}) \mathbf{w}_i^T \mathbf{x} - s_i(\mathbf{x}) b_i.$$

The output of the neural network can be written as

$$\begin{aligned} y(\mathbf{x}) &= \mathbf{w}_0^T \mathbf{a} = \sum_{i=1}^M s_i(\mathbf{x}) w_0[i] \mathbf{w}_i^T \mathbf{x} - \sum_{i=1}^M s_i(\mathbf{x}) w_0[i] b_i \\ &= \mathbf{w}_{\text{eq}}(\mathbf{x})^T \mathbf{x} - b_{\text{eq}}(\mathbf{x}). \end{aligned}$$

where

$$\mathbf{w}_{\text{eq}}(\mathbf{x}) = \sum_{i=1}^M s_i(\mathbf{x}) w_0[i] \mathbf{w}_i, \quad b_{\text{eq}}(\mathbf{x}) = \sum_{i=1}^M s_i(\mathbf{x}) w_0[i] b_i.$$

This locally linear model extends to any standard neural network, since convolutions and subsampling are inherently linear and max-pooling units can also be modeled as switches. For more than 2 classes, we will apply this modeling approach to the “transfer function” from the input to the inputs to the softmax layer, as discussed in Section 3.6.

3.3 Impact of adversarial perturbation

Now we consider the effect of an ℓ_∞ -bounded perturbation \mathbf{e} on the performance of the network. For ease of notation, we write $\mathbf{w}_{\text{eq}} = \mathbf{w}_{\text{eq}}(\mathbf{x})$, $\bar{\mathbf{w}}_{\text{eq}} = \mathbf{w}_{\text{eq}}(\mathbf{x} + \mathbf{e})$, and $\bar{b}_{\text{eq}} = b_{\text{eq}}(\mathbf{x} + \mathbf{e})$. The distortion due to the attack can be written as

$$\begin{aligned} \Delta &= y(\mathbf{x} + \mathbf{e}) - y(\mathbf{x}) \\ &= \bar{\mathbf{w}}_{\text{eq}}^T (\mathbf{x} + \mathbf{e}) - \bar{b}_{\text{eq}} - \mathbf{w}_{\text{eq}}^T \mathbf{x} + b_{\text{eq}} \\ &= \bar{\mathbf{w}}_{\text{eq}}^T \mathbf{e} + \left[(\bar{\mathbf{w}}_{\text{eq}} - \mathbf{w}_{\text{eq}})^T \mathbf{x} - (\bar{b}_{\text{eq}} - b_{\text{eq}}) \right] \end{aligned} \quad (1)$$

We observe that the distortion can be split into two terms: (i) $\bar{\mathbf{w}}_{\text{eq}}^T \mathbf{e}$ that is identical to the distortion for a linear classifier, and can be analyzed within the theoretical framework of Section 3.1 and (ii) $(\bar{\mathbf{w}}_{\text{eq}} - \mathbf{w}_{\text{eq}})^T \mathbf{x} - (\bar{b}_{\text{eq}} - b_{\text{eq}})$, that is determined by the ReLU units that flip due to the perturbation.

In the next section, we provide an analytical characterization of a “high SNR” regime in which the number of flipped switches is small, motivated by iterative attacks which gradually build up attack strength over a large number of iterations (with a per-iteration ℓ_∞ -budget of $\delta \ll \epsilon$). When very few switches flip, the distortion is dominated by the first term in (1), and we can apply our prior results on linear classifiers to infer the efficacy of the sparsifying front end in attenuating the distortion. As we discuss via our numerical results, this creates a situation in which it might sometimes be better (depending on dataset and attack budget) for the adversary to try to make the most of network’s nonlinearity, spending the attack budget in one go trying to flip a larger number of switches in order to try to maximize the impact of the second term in (1).

3.4 Characterizing the high SNR regime

We now investigate the conditions that guarantee high SNR at neuron i , i.e. $\bar{s}_i = s_i$, where \bar{s}_i denotes the switch when the adversary is present.

We observe that

$$\bar{s}_i = \begin{cases} 1 - s_i, & \mathbf{w}_i^T \mathbf{x} - b_i \in [\min(-\mathbf{w}_i^T \mathbf{e}, 0), \max(-\mathbf{w}_i^T \mathbf{e}, 0)] \\ s_i, & \mathbf{w}_i^T \mathbf{x} - b_i \notin [\min(-\mathbf{w}_i^T \mathbf{e}, 0), \max(-\mathbf{w}_i^T \mathbf{e}, 0)], \end{cases}$$

This implies the following sufficient condition for high SNR at neuron i : $|\mathbf{w}_i^T \mathbf{x} - b_i| > |\mathbf{w}_i^T \mathbf{e}|$.

Assumptions. To establish our theoretical result, we make a few mild technical assumptions:

1. The data is normalized in ℓ_2 -norm and bounded: $\|\mathbf{x}\|_2 = 1$ and $\|\mathbf{x}\|_\infty = \mathcal{O}(1)$.
2. The ℓ_∞ budget $\delta \leq |b_i|/\|\mathbf{w}_i\|_1 - C \ \forall i = 1, \dots, M$ and for some $C = \Theta(1) > 0$. Note that this assumption is justified in an iterative/optimization-based attack, where the adversary gradually spends the budget over many iterations.
3. The number of neurons $M = \omega(1)$ as N gets large.
4. For each neuron $i = 1, \dots, M$, we model the $\{w_i[k], k = 1, \dots, N\}$ as i.i.d, with zero mean $\mathbb{E}[w_i[k]] = 0$. We assume that $\mathbb{E}[w_i[k]^2] = \sigma_i^2 = \Theta(1)$.

Theorem 1. *With high probability, the high SNR condition ($\bar{\mathbf{s}} = \mathbf{s}$) holds for $1 - \mathcal{O}(1)$ fraction of neurons, i.e.*

$$\lim_{N \rightarrow \infty} \Pr\left(\frac{|S|}{M} = 1 - \mathcal{O}(1)\right) = 1,$$

where $S = \{i : |\mathbf{w}_i^T \mathbf{x} - b_i| > |\mathbf{w}_i^T \mathbf{e}|\}$.

Proof. We first state the following lemma:

Lemma 1. $\mathbf{w}_i^T \mathbf{x} \rightarrow \mathcal{N}(0, \sigma_i^2)$ in distribution.

Proof. We show that we can apply Lindeberg's version of the CLT, noting that $\mathbf{w}_i^T \mathbf{x} = \sum_{j=1}^N U_j$ is the sum of independent random variables, where $U_j = x_j w_i[j]$ with $\mathbb{E}[U_j] = 0$, $\text{var}(U_j) = \sigma_i^2 x_j^2$ and $\sum_{j=1}^N \sigma_i^2 x_j^2 = \sigma_i^2$.

Now given a constant $c_1 = \Theta(1) > 0$, we investigate the following quantity in order to check the Lindeberg condition:

$$L(c_1, N) = \frac{1}{\sigma_i^2} \sum_{j=1}^N \mathbb{E}\left[U_j^2 \mathbb{1}_{\{|U_j| > c_1 \sigma_i\}}\right]$$

From the assumptions on \mathbf{w}_i and \mathbf{x} , we observe that

$$\begin{aligned} \mathbb{E}\left[x_j^2 w_i^2[j] \mathbb{1}_{\{|U_j| > \delta \sigma_i\}}\right] &\leq \mathcal{O}^2(1) \Theta(1) \Pr(|U_j| > c_1 \sigma_i) \\ &= \mathcal{O}^2(1) \Theta(1) \Pr\left(|w_i[j]| > \frac{c_1 \sigma_i}{\mathcal{O}(1)}\right) \end{aligned}$$

The ℓ_∞ assumption on \mathbf{w}_i also implies that $\forall c_1 > 0, \exists N_0$ s.t. $|w_i[j]| < c_1 \sigma_i / \mathcal{O}(1), \forall j \in \{1, \dots, N\}, N > N_0$. Hence we obtain that $\lim_{N \rightarrow \infty} L(\delta, N) = 0$, which verifies the Lindeberg condition. \square

Noting that $\mathbf{w}_i^T \mathbf{x} - b_i \rightarrow \mathcal{N}(-b_i, \sigma_i^2)$, we can now write

$$\begin{aligned}
\Pr(|\mathbf{w}_i^T \mathbf{x} - b_i| > |\mathbf{w}_i^T \mathbf{e}|) &\geq \Pr(|\mathbf{w}_i^T \mathbf{x} - b_i| > \delta \|\mathbf{w}_i\|_1) \\
&= \Pr(\mathbf{w}_i^T \mathbf{x} - b_i > \delta \|\mathbf{w}_i\|_1) + \Pr(\mathbf{w}_i^T \mathbf{x} - b_i < -\delta \|\mathbf{w}_i\|_1) \\
&= Q\left(\frac{\delta \|\mathbf{w}_i\|_1 + b_i}{\sigma_i}\right) + Q\left(\frac{\delta \|\mathbf{w}_i\|_1 - b_i}{\sigma_i}\right) \\
&\geq Q\left(\frac{\delta \|\mathbf{w}_i\|_1 - |b_i|}{\sigma_i}\right) = Q\left(\frac{\|\mathbf{w}_i\|_1}{\sigma_i} \left(\delta - \frac{|b_i|}{\|\mathbf{w}_i\|_1}\right)\right) \\
&= Q\left(\Theta(N) \left(\delta - \frac{|b_i|}{\|\mathbf{w}_i\|_1}\right)\right) \rightarrow 1 \quad \text{as } N \rightarrow \infty,
\end{aligned}$$

where $Q(x) = \frac{1}{\sqrt{2\pi}} \int_x^\infty e^{-t^2/2} dt$ and $\delta < \frac{|b_i|}{\|\mathbf{w}_i\|_1}$ by Assumption 2. The theorem follows by using a union bound over $i = 1, \dots, M$. \square

3.5 Attacks

We assume that the adversary knows the true label, a reasonable (mildly pessimistic) assumption given the high accuracy of modern neural networks. We consider attacks that focus on maximizing the first term in (1), using a high SNR approximation to the distortion:

$$\Delta = y(\hat{\mathbf{x}}) - y(\mathbf{x}) = \mathbf{w}_{\text{eq}}^T \mathcal{P}_K(\mathbf{e}, \mathbf{x}) = \mathbf{e}^T \mathcal{P}_K(\mathbf{w}_{\text{eq}}, \mathbf{x}),$$

Here $\mathbf{w}_{\text{eq}} \approx \mathbf{w}_{\text{eq}}(\mathbf{x}) = \sum_{i=1}^M s_i w_0[i] \mathbf{w}_i$ if we are applying a small perturbation to the input data. However, for iterative attacks with multiple small perturbations, \mathbf{w}_{eq} would evolve across iterations.

We can now define attacks in analogy with those for linear classifiers. The adversary can use an ‘‘effective input’’ \mathbf{x}_1 to compute the locally linear model $\mathbf{w}_{\text{eq}} = \mathbf{w}_{\text{eq}}(\mathbf{x}_1)$. For example, the adversary may choose $\mathbf{x}_1 = \mathbf{x}$ if making a small perturbation, or may iterate computation of its perturbation using $\mathbf{x}_1 = \mathbf{x} + \mathbf{e}$. The adversary can also use a possibly different ‘‘effective input’’ \mathbf{x}_2 to estimate the set of basis coefficients retained by the sparse front ends. Armed with this notation, we can define two attacks:

$$\text{Semi-white box: } A_{\text{SW}}(\mathbf{x}_1, \epsilon) = \epsilon \text{sgn}(\mathbf{w}_{\text{eq}}(\mathbf{x}_1)),$$

$$\text{White box: } A_{\text{W}}(\mathbf{x}_1, \mathbf{x}_2, \epsilon) = \epsilon \text{sgn}(\mathcal{P}_K(\mathbf{w}_{\text{eq}}(\mathbf{x}_1), \mathbf{x}_2)).$$

We make no claims on the optimality of these attacks. They are simply sensible strategies based on the locally linear model, and as we show in the next section, they are more powerful than existing FGSM attacks for multiclass classification.

For simplicity, we set $\mathbf{x}_1 = \mathbf{x}_2$ for the white box attack, and simplify notation by denoting it by $A_{\text{W}}(\mathbf{x}_1, \epsilon)$. A (suboptimal) default choice is to set $\mathbf{x}_1 = \mathbf{x}_2 = \mathbf{x}$, relying on a high SNR approximation for both the network switches and for the sparsifying front end. However, we can also refine these choices iteratively, as follows.

Iterative versions: We choose a particularly simple approach, in which we use a small attack budget δ to change \mathbf{w}_{eq} by small amounts and update the ‘‘direction’’ of

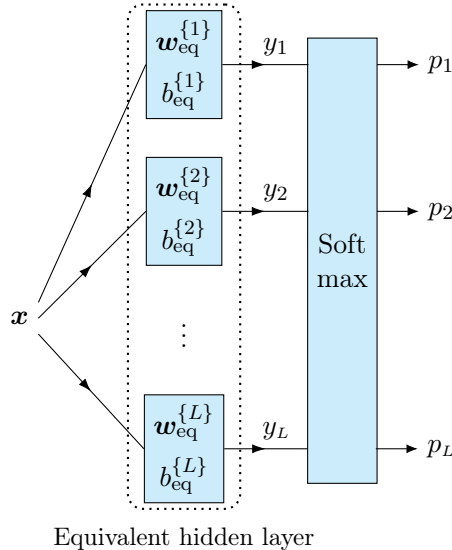


Figure 4: Multilayer (deep) neural network with L classes. Each of the L pre-softmax outputs (logits) is locally linear: $y_i = \mathbf{w}_{\text{eq}}^{\{i\}T} \mathbf{x} - b_{\text{eq}}^{\{i\}}$, $i = 1, \dots, L$.

the attack, maintaining the overall ℓ_∞ constraint at each stage:

$$\begin{aligned} \mathbf{e}_{k+1} &= \mathbf{e}_k + A(\mathbf{x} + \mathbf{e}_k, \delta) \\ \mathbf{e}_{k+1} &= \text{clip}_\epsilon(\mathbf{e}_{k+1}), \end{aligned}$$

where $\text{clip}_\epsilon(\mathbf{e}) \triangleq \max(\min(\mathbf{e}, \epsilon), -\epsilon)$. We believe there is room for improvement in how we iterate, but this particular choice suffices to illustrate the power of locally linear modeling.

Remark. The Fast Gradient Sign Method (FGSM) attack puts its attack budget along the gradient of the cost function $J(\cdot)$ used to train the network. For binary classification and the cross-entropy cost function, we can show that it is equivalent to the semi-white box attack with $\mathbf{x}_1 = \mathbf{x}$. Specifically, we can show that

$$\mathbf{e}_{\text{FGSM}} = \epsilon \text{sgn}(\nabla_{\mathbf{x}} J(\mathbf{x}, l)) = A_{\text{SW}}(\mathbf{x}, \epsilon)$$

where l is the true label, by verifying that the gradient is proportional to $\mathbf{w}_{\text{eq}}(\mathbf{x})$. For a larger number of classes, however, insights from our locally linear modeling can be used to devise more powerful attacks than FGSM.

3.6 Multiclass classification

In this subsection, we consider a multilayer (deep) network with L classes. Each of the outputs of the network can be modeled using the analysis in the previous section as follows:

$$y_i = \mathbf{w}_{\text{eq}}^{\{i\}T} \mathbf{x} - b_{\text{eq}}^{\{i\}}, \quad i = 1, \dots, L,$$

where $\mathbf{y} = [y_1, y_2, \dots, y_L]^T$, $p_i = S_i(\mathbf{y})$, and the softmax function $S_i(\mathbf{y}) = e^{y_i} / (\sum_{j=1}^L e^{y_j})$. Assume that \mathbf{x} belongs to class t (with label t known to the adversary).

Locally linear attack: The adversary can sidestep the nonlinearity of the softmax layer, since its goal is simply to make $y_i > y_t$ for *some* $i \neq t$. Thus, the adversary can consider $L - 1$ binary classification problems, and solve for perturbations aiming to maximize $y_i - y_t$ for each $i \neq t$. We now apply the semi-white and white box attacks, and their iterative versions, to each pair, with $\mathbf{w}_{\text{eq}} = \mathbf{w}_{\text{eq}}^{\{i\}} - \mathbf{w}_{\text{eq}}^{\{t\}}$ being the equivalent locally linear model from the input to $y_i - y_t$. After computing the distortions for each pair, the adversary applies its attack budget to the *worst-case* pair for which the distortion is the largest:

$$\max_{i,e} y_i(\mathbf{x} + \mathbf{e}) - y_t(\mathbf{x} + \mathbf{e}), \quad \text{s.t.} \quad \|\mathbf{e}\|_\infty \leq \epsilon$$

FGSM: Unfortunately, the FGSM attack does not have a clean interpretation in the multiclass setting. Taking the gradient of the cross-entropy between one-hot encoded vector of the true label \mathbf{l} ($l[k] = \delta_{tk}$) and the final output of the model $\mathbf{p} = [p_1, p_2, \dots, p_L]$, with $J(\mathbf{l}, \mathbf{p}) = -\sum_{i=1}^L l_i \log(p_i)$, we obtain

$$\mathbf{e}_{\text{FGSM}} = \epsilon \operatorname{sgn} \left(\mathbf{w}_{\text{eq}}^{\{t\}}(p_t - 1) + \sum_{k \neq t} \mathbf{w}_{\text{eq}}^{\{k\}} p_k \right).$$

This does not take the most direct approach to corrupting the desired label, unlike our locally linear attack, and is expected to perform worse.

4 Network sparsity

While the locally linear model for the entire network provides excellent guidance for both attack and defense, taking a more granular view by imposing sparsity *within* the network can yield further benefits in terms of robustness. We report here some preliminary results which show the promise of this approach.

Consider a neural network with ReLU nonlinearities $r(y) = \max(0, y)$. We note upfront the following Lipschitz property: $|r(y + \Delta y) - r(y)| \leq |\Delta y|$. For a vector argument, the ReLU nonlinearity is applied component-wise. Let \mathbf{x}_{j-1} denote the input to layer j and \mathbf{x}_j the output, with the original input denoted by $\mathbf{x}_0 = \mathbf{x}$. The output of the i th neuron at layer j is given by $x_j[i] = r(\mathbf{w}_{ij}^T \mathbf{x}_{j-1} - b_{ij})$.

Let us now apply an input perturbation \mathbf{e}_0 , so that the input to the neural network is $\bar{\mathbf{x}}_0 = \mathbf{x} + \mathbf{e}_0$. Denote by $\bar{\mathbf{x}}_j$ the corresponding outputs for layer j , $j \geq 1$, and set $\mathbf{e}_j = \bar{\mathbf{x}}_j - \mathbf{x}_j$ as the effective perturbation at the output of layer j . We can now state the following theorem on the implications of imposing network-level sparsity:

Theorem 2. *Consider an ℓ_∞ -constrained input perturbation $\mathbf{e}_0 = \mathbf{e}$, with $\|\mathbf{e}\|_\infty \leq \epsilon$. Suppose that we impose ℓ_1 constraints on the weights at each layer as follows:*

$$\|\mathbf{w}_{ij}\|_1 \leq \gamma_j \quad \forall i$$

Then the effect of the perturbation is ℓ_∞ -bounded at each layer:

$$\|\mathbf{e}_j\|_\infty \leq \epsilon \prod_{l=1}^j \gamma_l \tag{2}$$

Proof. The proof follows from application of Holder’s inequality at each layer, and noting the Lipschitz property of the ReLU nonlinearity. For the i th output neuron at the j th layer, we have

$$e_j[i] = \bar{x}_j[i] - x_j[i] = r(\mathbf{w}_{ij}^T(\mathbf{x}_{j-1} + \mathbf{e}_{j-1}) - b_{ij}) - r(\mathbf{w}_{ij}^T\mathbf{x}_{j-1} - b_{ij})$$

Setting $y_{ij} = \mathbf{w}_{ij}^T\mathbf{x}_{j-1}$ and $\Delta y_{ij} = \mathbf{w}_{ij}^T\mathbf{e}_{j-1}$, we note that $|\Delta y_{ij}| \leq \|\mathbf{w}_{ij}\|_1\|\mathbf{e}_{j-1}\|_\infty \leq \gamma_j\|\mathbf{e}_{j-1}\|_\infty$, where the first inequality follows from Holder’s inequality, and the second from the assumption of weight sparsity. We can now use the Lipschitz condition to note that

$$|e_j[i]| = |r(y_{ij} + \Delta y_{ij}) - r(y_{ij})| \leq |\Delta y_{ij}| \leq \gamma_j\|\mathbf{e}_{j-1}\|_\infty$$

Taking the maximum over i , we obtain that

$$\|\mathbf{e}_j\|_\infty \leq \gamma_j\|\mathbf{e}_{j-1}\|_\infty \tag{3}$$

Noting that $\|\mathbf{e}_0\|_\infty \leq \epsilon$, we can now apply the recursion (3) to obtain the desired layer-wise ℓ_∞ bounds specified in (2). \square

The theorem shows that, by imposing sparsity at each layer, we can control the worst-case growth of an adversarial perturbation as it flows up the network. Such sparsity can be imposed by incorporating ℓ_1 -regularization into backpropagation-based training. The details of how best to do this remain wide open, but we report here on some promising preliminary results for a two-layer fully connected network.

5 Experimental results

We perturb images with the following ℓ_∞ -bounded attacks in the white-box setting²:

- Locally linear attack.
- FGSM (Goodfellow et al., 2015).
- Iterative FGSM (Kurakin et al., 2017).
- Projected Gradient Descent (PGD) (Madry et al., 2018).
- Momentum Iterative FGSM, winner of the NIPS 2017 competition on adversarial attacks and defenses (Dong et al., 2017; Kurakin et al., 2018).
- Carlini-Wagner ℓ_2 attack (Carlini and Wagner, 2017).

In order to keep the focus on obtaining fundamental insight, we restrict attention to simple datasets: MNIST and Fashion-MNIST (LeCun et al., 1998; Xiao et al., 2017) and small networks: a 4-layer CNN and a 2-layer fully connected network.

² It was recently pointed out that several defenses rely on obfuscated gradients (Athalye et al., 2018) to circumvent white box attacks. We ensure that this does not happen by providing the gradient across the front end to the attacks. The gradient to be propagated is simply the projection onto the top K basis vectors of the input.

Table 1: Multiclass classification accuracies (4-layer CNN, MNIST)

	No defense	Sparsifying front end
Locally linear attack	8.82	79.48
FGSM	19.42	84.39
Iterative FGSM	0.58	50.48
Momentum Iterative FGSM	0.61	47.00
PGD	0.54	49.95

5.1 Setup

For multiclass classification, we use a 4-layer CNN consisting of two convolutional layers (containing 20 and 40 feature maps, both with 5x5 local receptive fields) and two fully connected layers (containing 1000 neurons each, with dropout) (Nielsen, 2015). We use a fully connected network with 1 hidden layer (containing 10 neurons) for binary classification of digits “3” and “7” for MNIST, and the classes “T-Shirt” and “Pullover” for Fashion-MNIST.

For the sparsifying front end, we use the Cohen-Daubechies-Feauveau 9/7 wavelet (Cohen et al., 1992) and retrain the network with sparsified images for various sparsity levels ($\rho = K/N$). Network sparsity was implemented via ℓ_1 regularization of weights during training.

5.2 Results

Table 1 reports on multiclass classification accuracies for the 4-layer CNN, where the single-step attacks use an ℓ_∞ budget³ of $\epsilon = 0.25$, and the iterative attacks use $\delta = \epsilon/20$ for 80 iterations. Without any defense, a strong adversary can significantly degrade performance, reducing accuracy from 99.38% to 0.54% (PGD). In contrast, when a sparsifying front end is present ($\rho = 3\%$), the network robustness measurably improves, increasing accuracy to 47% in the worst-case scenario. We note that the locally linear attack is stronger than FGSM. Results for the C&W ℓ_2 attack (which does not conform to our ℓ_∞ bounds) can be found in the appendix.

Table 2 reports binary classification accuracies for the locally linear attack (with $\epsilon = 0.25$). Without any defense, accuracy reduces from 99.39% to 8.31% for MNIST, and 97.2% to 2.83% for Fashion-MNIST. We observe that network sparsity is the stronger of the two defenses for Fashion-MNIST (improving accuracy to 66.94% at sparsity level $\rho = 3\%$), while both defenses perform about the same for MNIST. Results on accuracies as a function of ϵ can be found in the appendix.

³Images are normalized in the range [0,1].

Table 2: Binary classification accuracies (2-layer fully connected NN)

	No defense	Sparse network	Sparsifying front end
MNIST	8.31	80.46	80.68
Fashion-MNIST	2.83	66.94	62.05

6 Conclusions

In this paper, we have made the case that sparsity is a crucial tool for limiting the impact of adversarial attacks on neural networks. We have also shown that a “locally linear” model for the network provides key design insights, both for devising and combating adversarial perturbations. Our proposed sparsifying front end makes an implicit assumption on the generative model for the data that we believe must hold quite generally for high-dimensional data, in order to evade the curse of dimensionality. Our preliminary exploration of the complementary approach of weight sparsification, which can be trained in a purely discriminative manner, also shows promise. We believe that these results are the first steps towards establishing a comprehensive design framework, firmly grounded in theoretical fundamentals, for robust neural networks.

There are many directions for future research. Developing sparse generative models for various datasets is required for design of sparsifying front ends. For the simple datasets considered here, the orthogonal wavelet basis considered here was a good first guess, but it could be improved upon by learning from data, and by use of overcomplete bases. Our placeholder scheme of picking the largest K coefficients could be improved by devising computationally efficient and data-adaptive techniques for enforcing sparsity. A parallel track is to develop more detailed theoretical understanding and associated computational and training techniques for imposing network sparsity. It is also an open question as to how best to combine the “front-end” and “in-network” approaches. Finally, while we have restricted attention to simple datasets and small networks in this paper in order to develop insight, the design of larger (deeper) networks for more complex datasets is our ultimate objective.

References

- Athalye, A., Carlini, N., and Wagner, D. (2018). Obfuscated gradients give a false sense of security: Circumventing defenses to adversarial examples. In *International Conference on Machine Learning (ICML)*.
- Bhagoji, A. N., Cullina, D., Sitawarin, C., and Mittal, P. (2017). Enhancing robustness of machine learning systems via data transformations. *arXiv preprint arXiv:1704.02654*.
- Carlini, N. and Wagner, D. (2017). Towards evaluating the robustness of neural networks. In *IEEE Symposium on Security and Privacy*, pages 39–57.

- Cisse, M., Bojanowski, P., Grave, E., Dauphin, Y., and Usunier, N. (2017). Parseval networks: Improving robustness to adversarial examples. In *International Conference on Machine Learning (ICML)*, pages 854–863.
- Cohen, A., Daubechies, I., and Feauveau, J.-C. (1992). Biorthogonal bases of compactly supported wavelets. *Communications on Pure and Applied Mathematics*, 45(5):485–560.
- Das, N., Shanbhogue, M., Chen, S.-T., Hohman, F., Chen, L., Kounavis, M. E., and Chau, D. H. (2017). Keeping the bad guys out: Protecting and vaccinating deep learning with JPEG compression. *arXiv preprint arXiv:1705.02900*.
- Dong, Y., Liao, F., Pang, T., Hu, X., and Zhu, J. (2017). Discovering adversarial examples with momentum. *arXiv preprint arXiv:1710.06081*.
- Fawzi, A., Moosavi-Dezfooli, S.-M., Frossard, P., and Soatto, S. (2017). Classification regions of deep neural networks. *arXiv preprint arXiv:1705.09552*.
- Goodfellow, I. J., Shlens, J., and Szegedy, C. (2015). Explaining and harnessing adversarial examples. In *International Conference on Learning Representations (ICLR)*.
- Guo, C., Rana, M., Cisse, M., and van der Maaten, L. (2018). Countering adversarial images using input transformations. In *International Conference on Learning Representations (ICLR)*.
- Hein, M. and Andriushchenko, M. (2017). Formal guarantees on the robustness of a classifier against adversarial manipulation. In *Advances in Neural Information Processing Systems (NIPS)*, pages 2263–2273.
- Ilyas, A., Jalal, A., Asteri, E., Daskalakis, C., and Dimakis, A. G. (2017). The robust manifold defense: Adversarial training using generative models. *arXiv preprint arXiv:1712.09196*.
- Kurakin, A., Goodfellow, I., and Bengio, S. (2017). Adversarial machine learning at scale. In *International Conference on Learning Representations (ICLR)*.
- Kurakin, A., Goodfellow, I., Bengio, S., Dong, Y., Liao, F., Liang, M., Pang, T., Zhu, J., Hu, X., Xie, C., et al. (2018). Adversarial attacks and defences competition. *arXiv preprint arXiv:1804.00097*.
- LeCun, Y., Bottou, L., Bengio, Y., and Haffner, P. (1998). Gradient-based learning applied to document recognition. *Proceedings of the IEEE*, 86(11):2278–2324.
- Madry, A., Makelov, A., Schmidt, L., Tsipras, D., and Vladu, A. (2018). Towards deep learning models resistant to adversarial attacks. In *International Conference on Learning Representations (ICLR)*.
- Makhzani, A. and Frey, B. (2014). k -Sparse autoencoders. In *International Conference on Learning Representations (ICLR)*.
- Marzi, Z., Gopalakrishnan, S., Madhow, U., and Pedarsani, R. (2018). Sparsity-based defense against adversarial attacks on linear classifiers. In *IEEE International Symposium on Information Theory (ISIT)*.

- Moosavi-Dezfooli, S.-M., Fawzi, A., and Frossard, P. (2016). DeepFool: A simple and accurate method to fool deep neural networks. In *IEEE Conference on Computer Vision and Pattern Recognition (CVPR)*, pages 2574–2582.
- Nielsen, M. A. (2015). *Neural Networks and Deep Learning*. Determination Press.
- Poole, B., Lahiri, S., Raghu, M., Sohl-Dickstein, J., and Ganguli, S. (2016). Exponential expressivity in deep neural networks through transient chaos. In *Advances in Neural Information Processing Systems (NIPS)*, pages 3360–3368.
- Raghunathan, A., Steinhardt, J., and Liang, P. (2018). Certified defenses against adversarial examples. In *International Conference on Learning Representations (ICLR)*.
- Samangouei, P., Kabkab, M., and Chellappa, R. (2018). Defense-GAN: Protecting classifiers against adversarial attacks using generative models. In *International Conference on Learning Representations (ICLR)*.
- Sinha, A., Namkoong, H., and Duchi, J. (2018). Certifying some distributional robustness with principled adversarial training. In *International Conference on Learning Representations (ICLR)*.
- Szegedy, C., Zaremba, W., Sutskever, I., Bruna, J., Erhan, D., Goodfellow, I., and Fergus, R. (2014). Intriguing properties of neural networks. In *International Conference on Learning Representations (ICLR)*.
- Wong, E. and Kolter, Z. (2018). Provable defenses against adversarial examples via the convex outer adversarial polytope. In *International Conference on Machine Learning (ICML)*.
- Xiao, H., Rasul, K., and Vollgraf, R. (2017). Fashion-MNIST: A novel image dataset for benchmarking machine learning algorithms. *arXiv preprint arXiv:1708.07747*.

Appendix

A Notation

Here we define the notations $\Theta(\cdot)$, $\mathcal{O}(\cdot)$, $\omega(\cdot)$, and $\mathcal{o}(\cdot)$. We have

- $f = \mathcal{O}(g)$ if and only if there exists a constant $C > 0$ such that $|f/g| < C$,
- $f = \Theta(g)$ if and only if there exist two constants $C_1, C_2 > 0$ such that $C_1 < |f/g| < C_2$,
- $f = \omega(g)$ if and only if there does not exist a constant $C > 0$ such that $|f/g| < C$, and
- $f = \mathcal{o}(g)$ if and only if $g = \omega(f)$.

B Additional experimental results

B.1 Binary classification accuracies as a function of ϵ

Figures 5 and 6 report on binary classification accuracies as a function of ϵ ; here the iterative attacks use $\delta = \epsilon/10$ for 10 iterations. When using the network sparsity defense alone, the locally linear semi-white box and white box attacks coincide, and are labelled “linear attack” in the figure. As shown in Section 3.5, FGSM is identical to the locally linear attack for binary classification, so we do not label it in the figure. Since Fashion-MNIST classification is the harder of the two tasks, adversarial perturbations are able to overwhelm it even with low ϵ ; however both defense mechanisms confer robustness to a considerable range of ϵ . We note that images are normalized to the range $[0, 1]$, so by the end of the chosen range of ϵ , perturbations are no longer visually imperceptible. We also note that the locally linear white box attack that we consider is relatively naive, operating under a high SNR assumption (Marzi et al., 2018), hence it is not guaranteed to perform better than the semi-white box attack at larger ϵ .

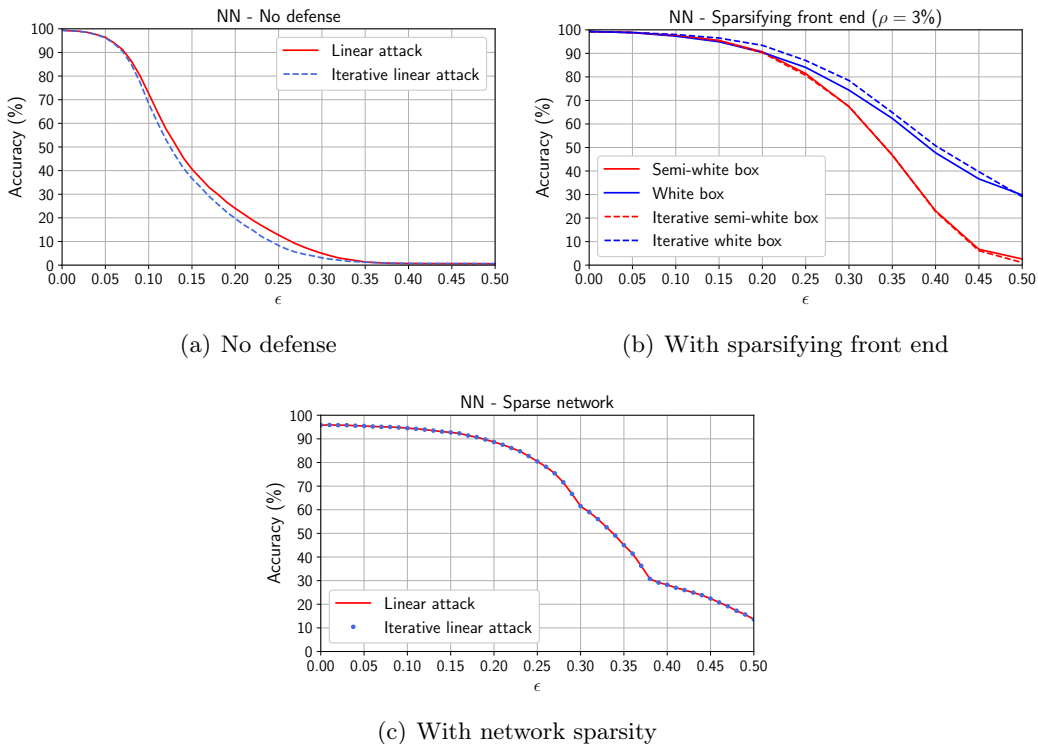


Figure 5: MNIST: Binary classification accuracies as a function of ϵ

B.2 Effect of sparsification on performance without attacks

In Figures 5 and 6, we report implicitly on the effect of sparsification on performance without attacks (the $\epsilon = 0$ points). Specifically, there is a slight performance hit: for MNIST, the accuracy goes from 99.37% to 98.4% (multiclass) and 99.39% to

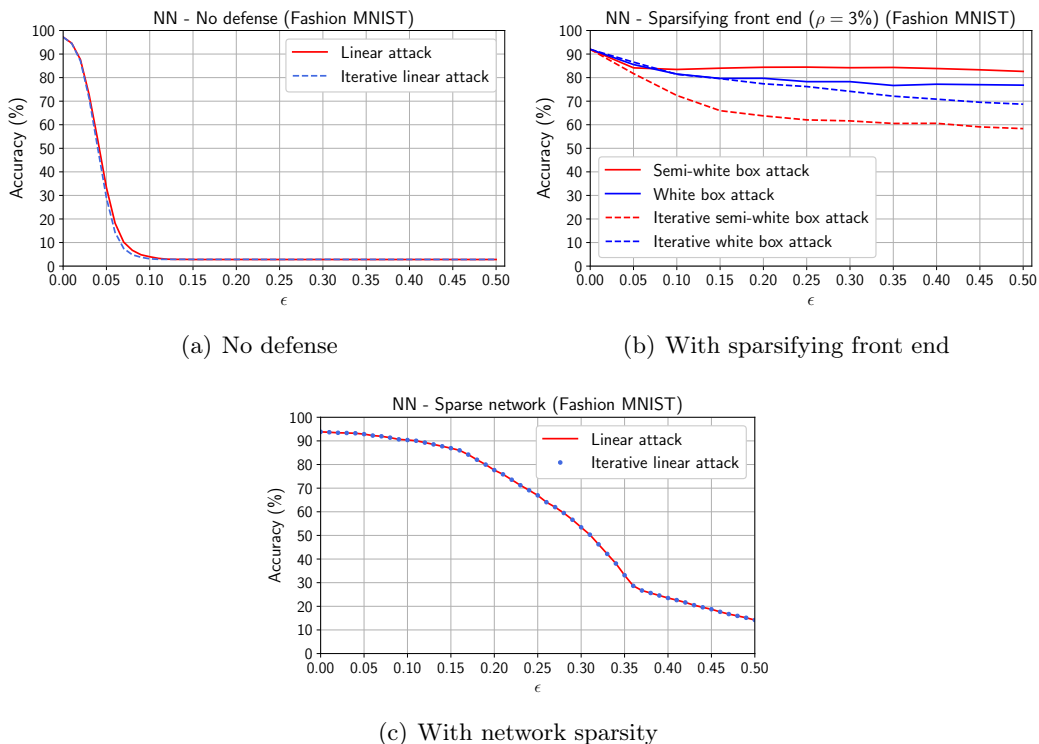


Figure 6: Fashion-MNIST: Binary classification accuracies as a function of ϵ

99.27% (binary). We note that sparsity has also been suggested purely as a means of improving classification performance (e.g., see Makhzani and Frey (2014)) and hence believe that with additional design effort, the performance penalty will be minimal.

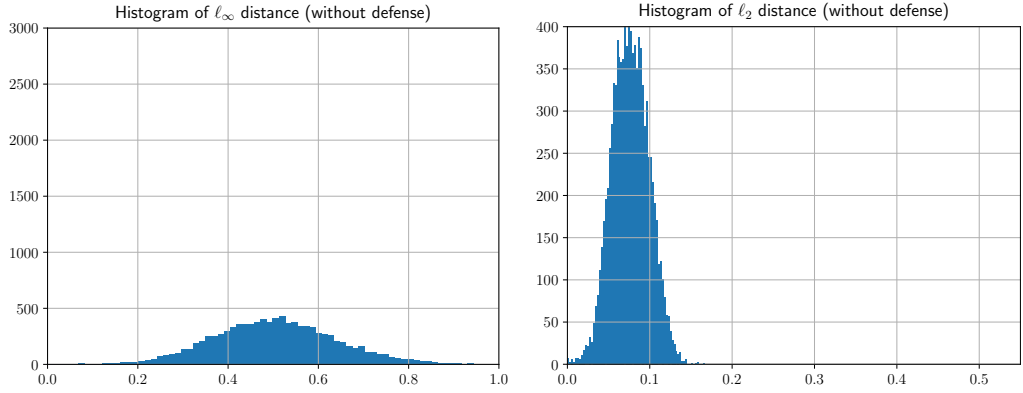
B.3 Experiments on the Carlini-Wagner ℓ_2 attack

Since the Carlini-Wagner attack does not have a fixed bound on the distance between adversarial and true images (Carlini and Wagner, 2017), we report on histograms of distances in Figure 7. We set the confidence level of the attack to 0; in the C&W attack formulation, this corresponds to the smallest possible ℓ_2 distance. The final classification accuracy is 4.05%, but 98% of the perturbed images lie outside the ℓ_∞ budget of interest⁴. We also note that the front end increases the average ℓ_2 distance by a factor of ~ 2.5 . The attack is successful in terms of causing misclassification, but since it is an ℓ_2 attack, it fails to produce perturbations conforming to the ℓ_∞ budget.

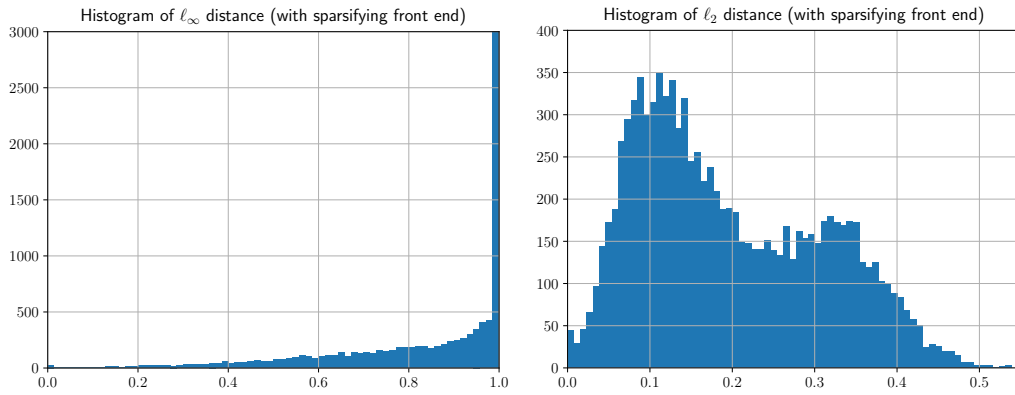
For computational efficiency reasons, we use a Backward Pass Differential Approximation (BPDA) (Athalye et al., 2018) of identity for the gradient of the sparsifying front end. The other attack hyperparameters are listed below:

$$\| \text{LEARNING_RATE} = 1\text{e-}2, \text{ INITIAL_CONST} = 1\text{e-}3, \text{ MAX_ITERATIONS} = 1000.$$

⁴ $\|e\|_\infty \leq 0.25$, with images normalized in the range $[0,1]$.



(a) Histogram of ℓ_∞ distance (without defense). Mean = 0.503. (b) Histogram of ℓ_2 distance (without defense). Mean = 0.076.



(c) Histogram of ℓ_∞ distance (with front end). Mean = 0.826. (d) Histogram of ℓ_2 distance (with front end). Mean = 0.196.

Figure 7: Histograms of adversarial examples generated by the C&W attack on the 4-layer CNN with sparsifying front end ($\rho = 3\%$).